JOURNAL OF MATERIALS SCIENCE 35 (2000) 1891–1900

An NMR microscopy study of water absorption in cork

A. M. GIL*
Departamento de Química, Universidade de Aveiro, 3800 Aveiro, Portugal
E-mail: agil@dq.ua.pt

M. H. LOPES, C. PASCOAL NETO
Departamento de Química, Universidade de Aveiro, 3800 Aveiro, Portugal

P. T. CALLAGHAN
Institute of Fundamental Sciences-Physics, Massey University, Palmerston North, New Zealand

NMR Microscopy is used to measure the imbibition of water into natural cork, extractives-free cork and desuberised cork. The results clearly indicate that suberin is the key constituent which determines the ability of cork to resist water uptake. Furthermore, a particular suberin with distinct spectral properties as viewed by ^{13}C NMR is shown to be the component responsible for cork resistance to water absorption. Laser confocal microscopy suggests that this function is associated with the role of suberin in preserving cell wall structure but the highly hydrophobic nature of suberin may also play an important role. The NMR microscopy study shows that the water absorbed by natural cork, after soaking for three days, is confined to the lenticels, narrow channels on the order of 1000 to 1500 μm in diameter. One incidental outcome is the observation of a clear down-field shift in NMR frequency for water near the cut transverse surfaces of the cork, an effect associated with susceptibility inhomogeneity.

1. Introduction

The material commonly known as cork is the outer bark of *Quercus suber* L. tree and comprises three main components: suberin (40% w/w), lignin (22% w/w) and carbohydrate (20% w/w) [1]. The remainder comprises waxes and other extractives. The unique functional properties of cork have lead to wide applications of this material in a variety of products such as stoppers, wall and floor materials.

Many studies have been carried out in order to fully characterise the structure of the major component of cork, suberin, which is believed to be a biopolyester composed mostly of aliphatic domains, mainly C16–C26 hydroxyacids, and possibly some aromatic domains [2–5]. Whereas the aliphatic nature of suberin has been established, the aromatic part of suberin has not yet been entirely characterised. Several studies suggest that it may be similar to that of lignin [6–10], i.e. interlinked monolignols and, in a recent study, the aromatic domain of potato, suberin has been proposed to be mainly composed of hydroxycinnamic acid derived polymeric matrix [11]. Suberin is also found in underground parts and wound surfaces of higher plants, where it is believed to act as an extracellular biological barrier, preventing the diffusion of water and/or other molecules [2].

The diffusion of water in cork is known to be a significantly slow process, as shown by a previous quantitative study carried out on the basis of mass and volume changes as a function of time [12]. It was found that it may take over 1 year for a 1 mm-thick cork plate to sink in water. The same authors have estimated water diffusion coefficients by measuring the changes in electrical resistance while water diffuses through cork. Such results were discussed with basis on the anisotropic cell structure of cork [12]. The two hydrophobic components of cork, suberin and extractives, are believed to be closely related to the impermeability of that material to water. Recent studies involving the measurement of surface energies for cork, extractives-free cork and desuberised cork suggested the importance of suberin in conferring hydrophobicity to cork [13, 14].

The present work aims at establishing the relative importance of each of the two hydrophobic components, extractives and suberin, in determining water-insulating properties. Rather than characterising the full and rather slow process of water absorption by cork, the water absorption occurring during a constant short period of time (3 days) was compared for 1) natural cork, 2) extractives-free cork and 3) partially desuberised cork. Desuberised cork was prepared in two ways: by non-selective suberin removal upon alkaline treatment and

* Author to whom all correspondence should be addressed.

by selective desuberisation under controlled heating conditions. The distribution of water in each sample was investigated non-invasively by ^{1}H Nuclear Magnetic Resonance (NMR) Microscopy and the results discussed with basis on both the chemical composition of the samples and the physical effects of the chemical treatments on the cell wall structure, as viewed by confocal microscopy.

NMR Microscopy is based on the principle that nuclear spins, immersed in a polarising magnetic field, experience a phase rotation (precession) whose frequency depends on the field strength. Of all nuclear spins present in atoms common to natural materials, the hydrogen proton is the most abundant and sensitive to NMR measurement. Consequently in all that follows, the proton is the "NMR nucleus" under investigation and, in particular, we shall be concerned with the signal arising from protons in water molecules.

In Nuclear Magnetic Resonance the nuclear spin is disturbed from thermal equilibrium by a pulse of oscillatory magnetic field whose frequency matches the nuclear spin precession. This pulse re-orients the spin magnetisation away from its equilibrium state longitudinal to the polarising field. The resulting "transverse magnetisation" freely precesses about the polarizing field and will induce a oscillatory emf in a receiver antenna placed around the sample. Gradual loss of phase coherence and the subsequent re-establishment of thermal equilibrium leads to relaxation of this transverse magnetisation (T_2 relaxation) and the restoration of the equilibrium longitudinal polarisation (T_1 relaxation).

Imaging of nuclear spin positions is possible by means of magnetic fields whose intensity vary in position. Suppose one applies a magnetic field of strength B_0 and, in addition, a magnetic field gradient $\mathbf{G} = \nabla \boldsymbol{B_0}$ (this can be achieved with specialised coil designs capable of generating quite uniform gradients along three orthogonal axes). In that case the nuclear precession frequency will depend on spin location and can be written

$$\omega = \gamma B_0 + \gamma \mathbf{G}\cdot\mathbf{r} \qquad (1)$$

Because the receiver uses heterodyne phase-sensitive detection with reference frequency γB_0, the additional term, $\gamma \mathbf{G}\cdot\mathbf{r}$, shows up as a difference oscillation, generally in the audio-frequency part of the spectrum. As a consequence the heterodyne signal detected via the NMR coil at time t after the spins have precessed in the gradient has the mathematical form [15]:

$$S(\mathbf{k}) = \int \rho(\mathbf{r}) \exp(\mathrm{i}2\pi \mathbf{k}\cdot\mathbf{r})\, \mathrm{d}\mathbf{r} \qquad (2)$$

where $\exp(\mathrm{i}2\pi\mathbf{k}\cdot\mathbf{r})$ is the local spin phase factor for the spins at position $\mathbf{r}$, $\mathbf{k} = (2\pi)^{-1}\gamma\mathbf{G}t$, and $\rho(\mathbf{r})$ is the density of spins at position $\mathbf{r}$ and is the quantity we seek to image. Equation 2 is a simple Fourier transform in which $\mathbf{k}$ is the reciprocal space wave vector conjugate to the spatial dimension $\mathbf{r}$. Acquisition of a signal in a domain of "k-space" leads to direct computation of $\rho(\mathbf{r})$ by means of Fourier inversion. Generally one acquires an image of the spin distribution in a 2-dimensional planar "slice", with a frequency-selective rf pulse being used to excite only spins within a pre-selected plane, and the k-space encoding being applied independently for two orthogonal directions within the plane, one direction via a fixed time duration variable magnitude gradient pulse (phase-encoding) and the other direction via a fixed gradient pulse with the signal being sampled at successive time points during the evolution (read-encoding). Further details of NMR Microscopy methods can be found in reference 15.

The pulse sequences used to obtain the images presented in this article are shown in Fig. 1. The first employs a spin echo in which a separate 180° rf pulse is used to invert spin phases. This allows one to traverse both negative and positive regions of k-space. The use of the spin echo means that the NMR signal is inevitably affected by T_2 relaxation since the nuclear

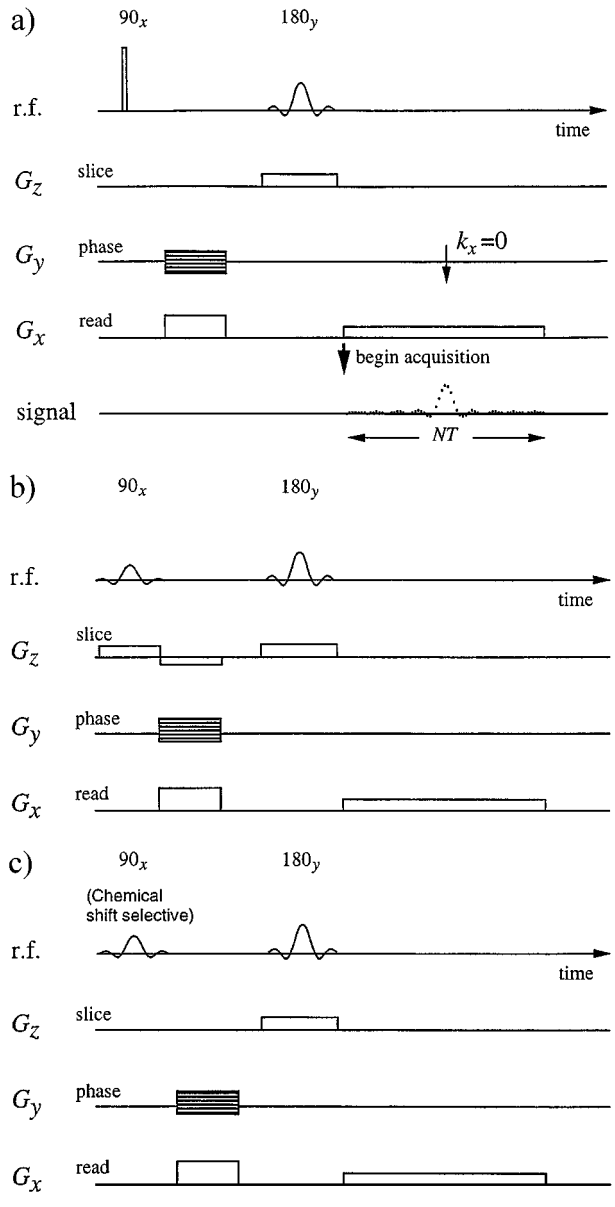

Figure 1 The pulse sequences used to obtain the images presented in this article. Fig. 1a shows the standard spin warp sequence while Fig. 1b and c show multi-slice and chemical shift selection sequences.

magnetisation is exposed to transverse relaxation over the echo time, T_E. T_2 is determined predominantly by internuclear interactions which in turn are motionally averaged by molecular tumbling. This means in effect that molecules in the liquid state have long proton T_2 values (10 to 1000 ms) while those in the solid state may have relaxation times as short as 10 μs. This results in a sharp discrimination of the signal in which the solid state component is entirely filtered out. In the results to be reported here the NMR image arises from protons in the mobile phase alone. In the second sequence, shown in Fig. 1b, the excitation and refocusing rf pulses are both selective and allow multiple and adjacent planes of the sample to be imaged by successively shifting the slice plane position, an effect achieved simply by shifting the rf pulse frequency. The third sequence illustrates the use of a "chemically-selective" excitation pulse and a slice-selective refocusing pulse. By this means an image may be acquired from differing parts of the NMR frequency spectrum.

It should be noted that the spatial resolution in NMR Microscopy is limited by the three factors of intrinsic signal-to-noise, molecular self diffusion and diamagnetic susceptibility effects. A description of the respective contributions is complex, beyond the scope of this article, and may be found in detail in reference 15. A practical limit to resolution for proton NMR microscopy is around 10 μm^3. However, when imaging water in most natural materials, proton T_2 values may be quite short and thereby limit the signal-to-noise ratio, thus degrading the available resolution considerably.

In order to establish the physical changes in cork cell structure arising from the chemical treatments employed in this work, some images of the samples studied were obtained by means of confocal laser microscopy. This technique relies on the laser-excitation of a fluorescing dye molecule attached to the sample being studied. The confocal optics ensures that the light collected by the microscope objective arises from a narrow focal plane, and in consequence, only a narrow slice of material is examined. The technique is described in some detail elsewhere [16].

2. Experimental

2.1. Sample preparation

Cork cylinders were cut out from a cork plank using a rotating metallic tube. The cylinders were cut to a 1–1.5 cm length along the tree radial direction and a diameter of 1 cm in the tangential direction. The terms tangential, axial and radial hereby used follow previous descriptions of the different directions of cellular growth in the cork tree [12]. Extractive components were separated by sequential soxhlet extractions with dichloromethane, ethanol and water, for 24 hours in each solvent.

The effects of two desuberisation processes, non-selective desuberisation and selective desuberisation, on water absorption were investigated. The first process was achieved by suberin depolymerisation by a 8 hours methanolysis treatment with 0.02% NaOMe [18]. This treatment has been shown to affect all types of aliphatic suberin to similar extents. A cylindrical sample of cork with 17% suberin (calculated relatively to 100 grams of cork) removed was obtained. Selective desuberisation was achieved by heating an extractive-free cork cylinder at 250°C for 20 min, conditions which have been reported to cause selective degradation and removal of the aliphatic suberin type which resonates at 33 ppm in the ^{13}C CP/MAS spectrum [19]. The sample was subsequently cooled to room temperature in a desiccator.

For the NMR studies, the cylinder-shaped samples of natural cork, cork without extractives and desuberised cork were immersed in water for 72 hours. The amount of absorbed water was estimated by weighting the samples before and after immersion. Excess water at the cylinder surface was removed by gently touching the surface with tissue paper.

For the confocal microscopy studies, the samples immersed in water for 72 hours were analysed after subsequent air-drying. These samples were compared with samples which had suffered the same chemical treatments but had not been immersed in water. The samples were prepared by cutting slices, approximately 1 mm thick, along the axial/tangential directions of the cylinders studied by spectroscopy. The slices were stained in a 1% aqueous acridine orange solution for 24–48 hours. Microscopic images were obtained for focal plane layers of around 40 μm thickness, in both the sections parallel (radial section) and perpendicular (tangential section) to the radial direction of the tree.

2.2. NMR microscopy and spectroscopy

All NMR Microscopy experiments were carried out at 22°C using a Bruker AMX 300 NMR spectrometer (Karlsruhe, Germany) with standard microimaging attachments. The cork samples were wrapped in teflon tape and placed in a 15 mm diameter resonator. The 128×128 pixel images were obtained from a 1 mm thick selectively excited slices using a 10 mm field of view. In order to minimize the echo time ($T_E = 3.6$ ms) we used the largest possible gradient amplitudes (0.35 T m^{-1}) corresponding to an acquisition spectral width of 120 kHz. Images were obtained in different orthogonal planes over a period of 7 minutes, using 4 signal averaging steps with a repetition time (T_R) of 800 ms. In multislicing experiments the adjacent slices were separated by 1.5 mm. In experiments using the "chemical shift" selective excitation scheme of Fig. 1c, the selective excitation pulse was a 5 ms duration gaussian with a bandwidth on the order of 200 Hz. Static ^1H NMR spectra were recorded with a spectral width of 10 kHz, a 90° pulse length of 18 μs, 4 accumulations and a 2 s recycle time.

The Magic Angle Spinning (MAS) ^1H NMR spectrum of a cylinder of natural cork, after immersion in water for 72 hours, was recorded on a Bruker MSL 400P spectrometer, operating at 400 MHz for protons. A rotation speed of 5 kHz was employed, together with a 3 μs 90° pulse length and a 5 s recycle delay. 400 accumulations were co-added. The effects of heating the cylinder of extractive free cork on its chemical composition

were checked by recording a ^{13}C Cross Polarisation and Magic Angle Spinning (CP/MAS) spectrum before and after the treatment. The cylinder was packed in a rotor and spun at 5 kHz and the ^{13}C CP/MAS spectrum was recorded with a contact time of 1 ms, a recycle delay of 4 s, a 90° pulse of 6 μs and the accumulation of 4796 scans.

2.3. Confocal microscopy

A Leica TCS 4D confocal microscope was used. A 400 times total magnification was used for all cork images, with a 40 times amplification objective with a 1.0 numerical aperture and an oil immersion lens. The light source used was an argon/krypton mixed gas laser which was tuned into a selected excitation wavelength of 488 nm. Emissions were registered for wavelengths greater than 590 nm.

3. Results and discussion

3.1. Natural cork

Fig. 2 shows a set of 6 adjacent image slices obtained, in the tangential section, from the cylindrical sample of natural cork which had been soaked in water for 3 days. Although a significant mass increase was registered for this cork sample (about 170%), it is clear from Fig. 2 that water is confined to channels with diameters between 1000 and 1500 μm which could be directly identified in a surface examination as being dark stained. These are the lenticular channels or lenticels whose number and size are closely related to the quality of cork [17]. The ability of cork cellular structure to resist water ingress is related to the closed cellular arrangement characterising the material. Confocal microscopy images of both tangential and radial sections of the same natural cork sample (Fig. 3a and b) showed a regular and continuous arrangement of cells in both sections, as it was observed before [12]. The effect of water absorption (and subsequent air-drying) on the cellular structure of natural cork was shown to result in a degree of cell corrugation (Fig. 4a), again in support of previous reports [12]. The cellular arrangement of cork provides, therefore, an efficient barrier to water ingression probably due to its closed, continuous nature and/or to the strong hydrophobic nature of the material, conferred by both extractives and suberin. The roles played by each of these factors will be investigated next.

Fig. 5a shows the static proton NMR spectrum of the soaked natural cork cylinder and the corresponding insert shows the ^{1}H MAS spectrum obtained for the same sample. As expected, both spectra are dominated by the water peak but some fine structure should be noted. Firstly, the static spectrum shows a significant number of overlapped peaks downfield of the water peak, the nature of which will be discussed below. Secondly, a high field shoulder may be observed in the ^{1}H MAS spectrum of the same sample, reflecting the high content of aliphatic suberin in cork and its relatively high mobility, compared to the remaining cell wall components [18]. Such peak is not observed in the static spectrum due to anisotropic linebroadening contributions.

The intriguing feature of the static NMR spectrum will now be discussed further. This spectrum is dominated by a peak a few kHz wide arising from the protons in molecular segments sufficiently mobile for the spin-spin relaxation time to be on the order of or greater

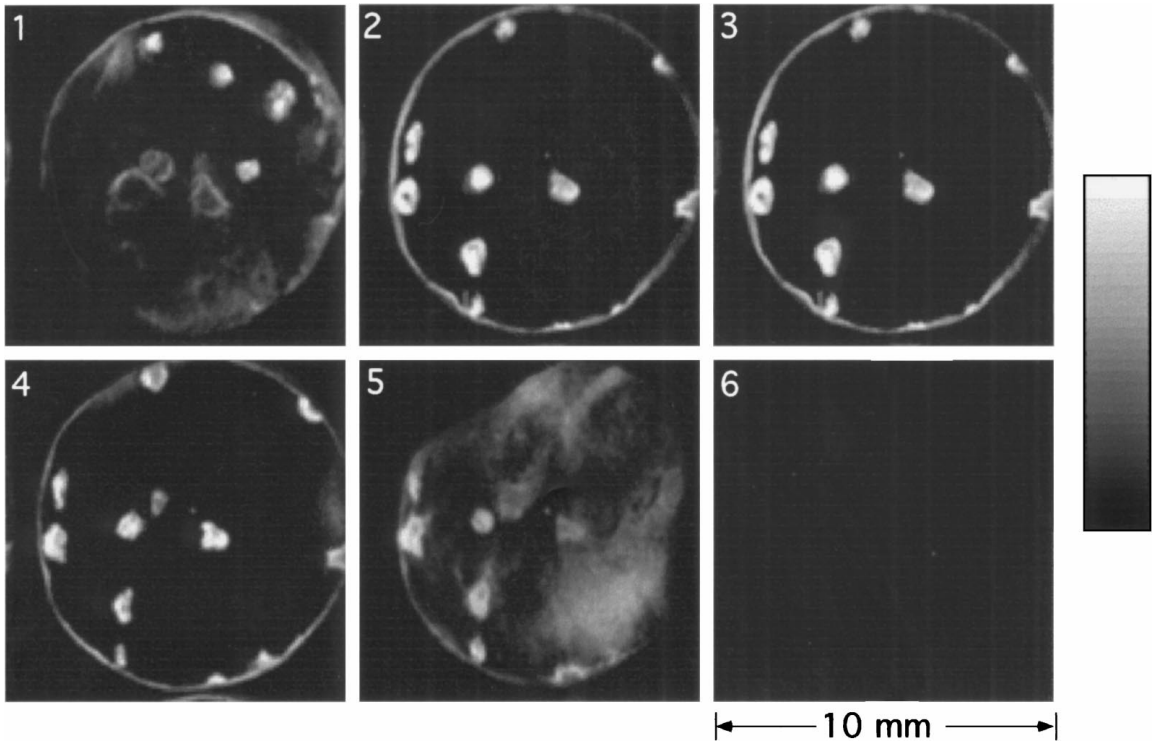

Figure 2 Set of 6 adjacent image slices obtained in tangential section of a sample of natural cork, after soaking in water for 72 hours. Each slice is 1 mm thick and separated from its neighbours by 1.5 mm. The images are sequential as numerically labelled. The bright regions correspond to water absorbed in lenticels while surface water is also apparent.

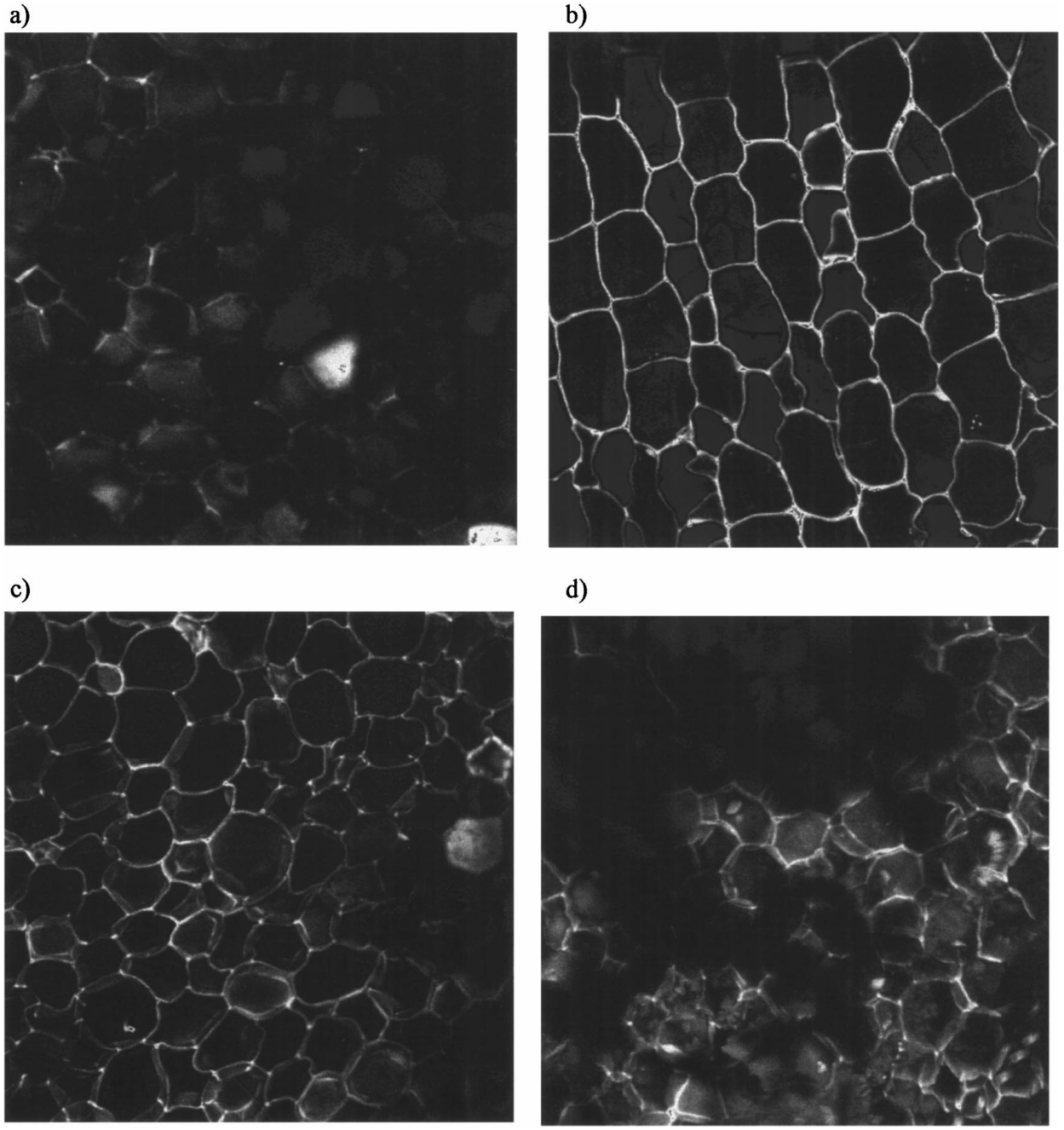

Figure 3 Confocal microscopic images of (a) tangential section and (b) radial section of natural cork, (c) tangential section of extractives-free cork, (d) tangential section of non-selectively desuberised cork (17% suberin removed). Scale: 1 cm corresponds to 20 μm.

than a few ms. We believe that all of this signal arises from absorbed water. This is confirmed by the observation that the low field peaks are no longer present under MAS conditions (Fig. 5a, insert), indicating that they originate from resonance frequency-shifted water, rather than from any of the cork components. Of course, by comparison with pure water, the spectrum shown in Fig. 5a is rather broad, and the rapid T_2 relaxation time (on the order of 5–30 ms), rather short. Fig. 6 shows an image of T_2 relaxation times (T_2 map) obtained for the natural cork sample, together with an intensity map obtained after correction for signal loss due to T_2 relaxation. It is clear that the water protons close to the cell walls have slightly shorter values (5–10 ms) whereas the bulk water present within each lenticular pore has T_2 values of 20–30 ms. These observations indicate a significant role played by surface interactions. Collision of water molecules with solid surfaces is known to reduce the spin-spin relaxation time, either by temporary immobilisation at the adsorbed layer, or by diffusion in the presence of strong local magnetic field gradients. These gradients arise from the structural heterogeneity and consequent strong diamagnetic susceptibility inhomogeneity. Such inhomogeneity also directly affects the NMR lineshape by shifting the NMR frequency by a small amount (on the order of a few ppm) depending on the local surface symmetry with respect to the magnetic field.

In order to characterise in more detail the nature of the lineshape structure observed downfield of the main peak, we have carried out a frequency selective experiment in which we obtaine separate images from the main peak in the NMR spectrum (at 4.7 ppm) and the low field component (at about 7.5 ppm). These are

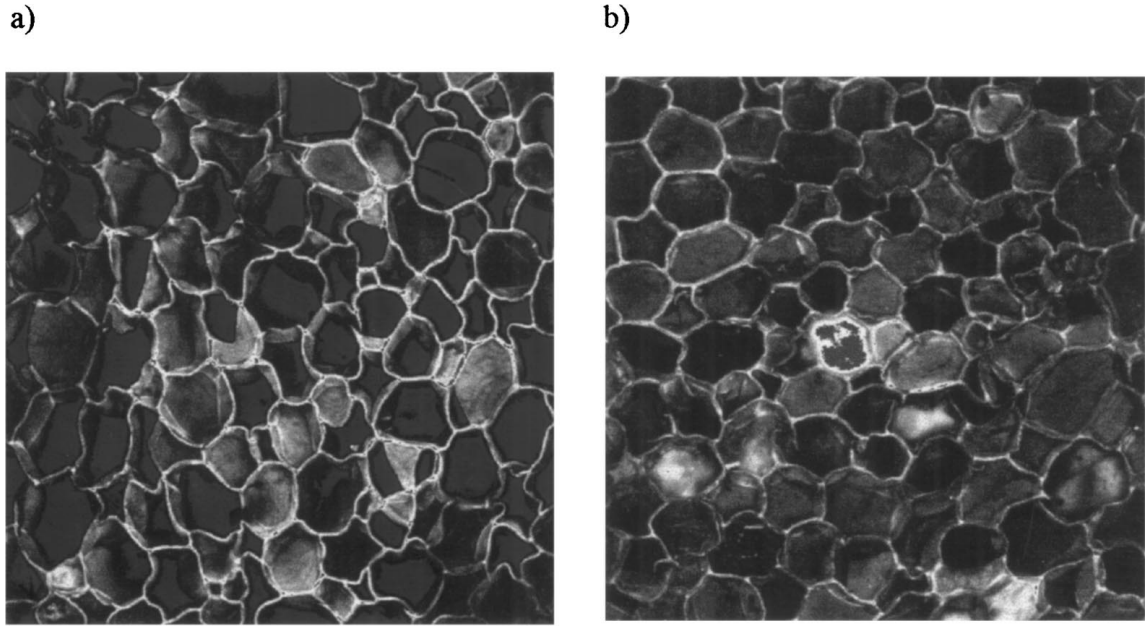

Figure 4 Confocal microscopic images of tangential sections of (a) natural cork, (b) extractives-free cork, after immersion in water for 3 days and subsequent air-drying. A satisfactory microscopic image of the non-selectively desuberised sample (17% suberin removed) could not be obtained (see text). Scale: 1 cm corresponds to 20 μm.

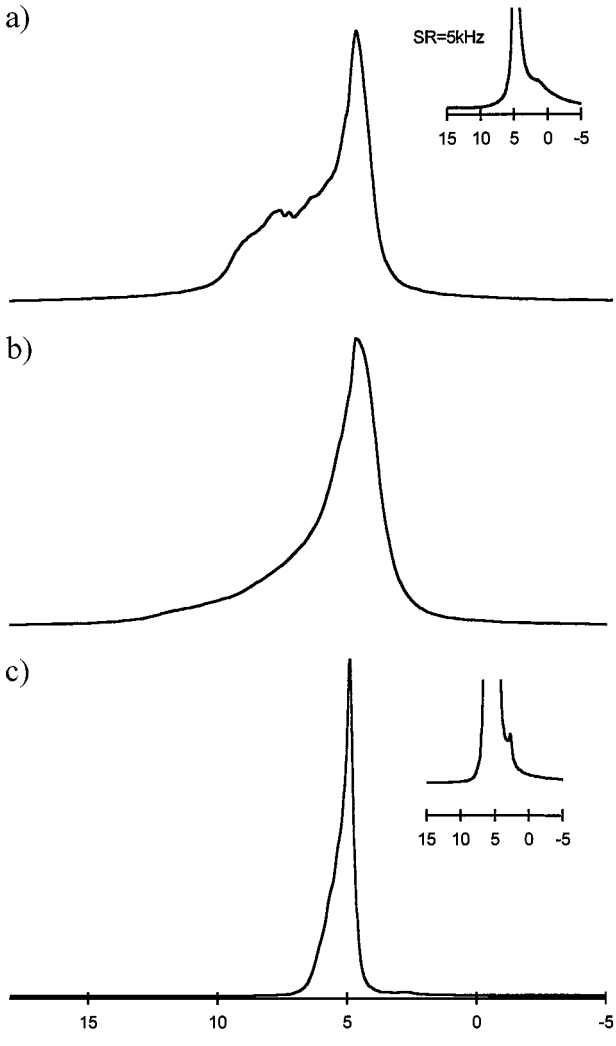

Figure 5 Static proton NMR spectra of soaked (a) natural cork (insert shows the ^{1}H MAS spectrum of the natural cork cylinder); (b) extractives-free cork; (c) non-selectively desuberised cork (insert shows expansion).

shown respectively in Fig. 7a and b while a superposition of the images in seen in Fig. 7c. The images suggest that the low field part of the spectrum arises from water located at the end of channels in the cork on the bottom and top faces of the cylindrical sample, an effect which we attribute to diamagnetic susceptibility effects at the air/water interface. These results show that such spectral contrast can be used to provide additional spatial definition, indeed that it is possible to obtain selective signals from water in differing regions of the cork sample, by NMR spectroscopy alone. Such an effect could provide a useful tool for monitoring initial water ingress at the cork surface by such spectroscopic means, without the need to directly image the sample via NMR Microscopy.

3.2. Extractives-free cork

Fig. 8 shows multislice images along the tangential and radial sections of the sample of extractive-free cork. It is clear from the figure that water is again confined to the lenticular channels, as in natural cork. The removal of extractives makes, therefore, little difference to the ability of cork to resist water ingress and, in fact, both natural and extractives-free cork show similar mass increases (about 170% w/w) due to water absorbed into the lenticels. Fig. 3c shows the confocal microscopy image of the tangential section of extractive-free cork, indicating that the effect of the treatment for extractives removal is merely to expand the cells slightly. The effect of water absorption and subsequent air-drying on the cellular structure of extractive-free cork (Fig. 4b) is very similar to that observed for natural cork (Fig. 4a) indicating that, in both cases, the cellular structure remains intact although showing signs of general corrugation. It may be concluded, therefore, that cork extractives

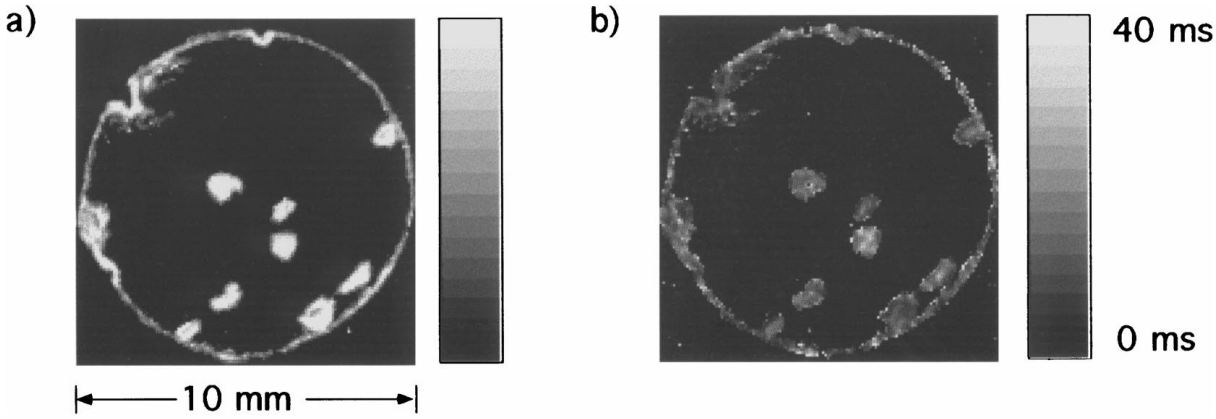

Figure 6 Images of (a) T_2 relaxation times (grey scale 0 ms to 40 ms) and (b) proton intensities, obtained for natural cork, after soaking in water for 72 hours.

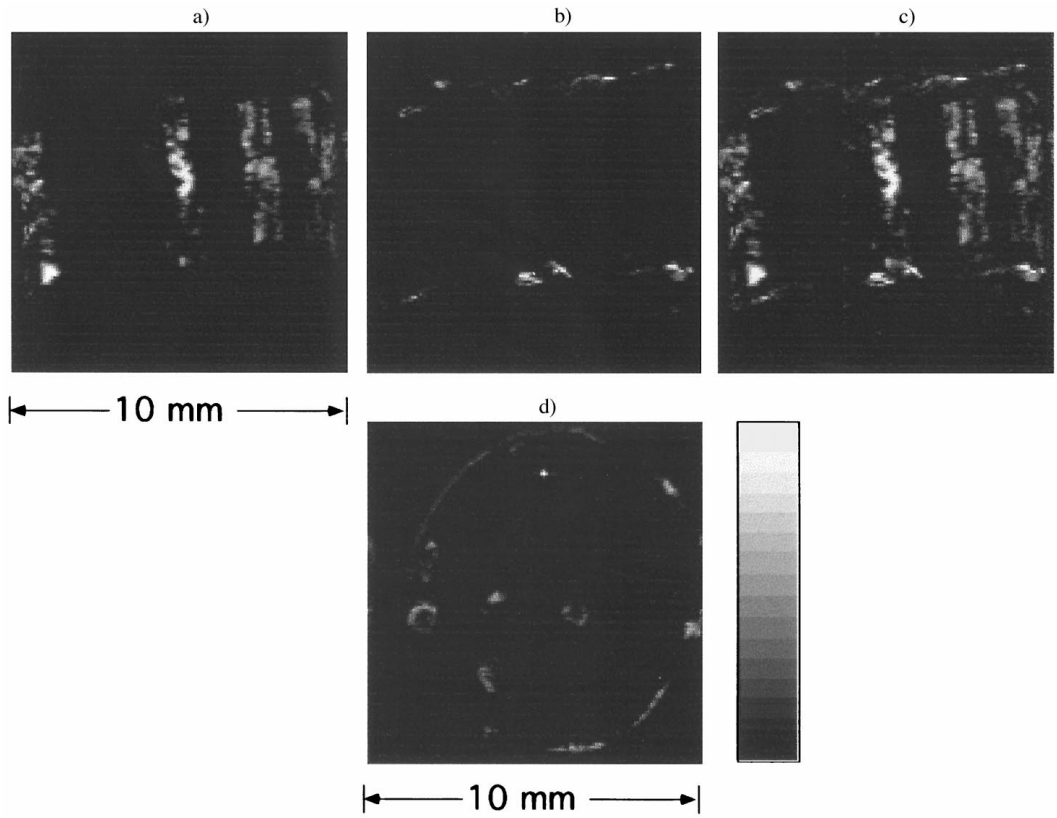

Figure 7 Proton intensity images obtained for natural cork, soaked for 72 hours with selection of (a) the water peak at 4.7 ppm and of (b) the low field signal at 7.5 ppm. (c) superposition of a) and b); (d) superposition image in tangential section.

not only do not play a significant role in the cellular structure, but also that their hydrophobic nature does not contribute markedly towards the water-insulating properties of cork [13, 14].

The static proton NMR spectrum of the sample of extractive-free cork (Fig. 5b) is, as expected, dominated by the water peak and, although some asymmetry is apparent, it is clear that the spread of water chemical shifts observed for natural cork (Fig. 5a) is absent. The absence of the downfield peaks was reproduced on a second sample of extractives-free cork, indicating that a different susceptibility effect occurs for the sample to which extractives were removed. The susceptibility effects on the water resonance are closely related to the shape of the water cylinder inside the lenticular channels and, particularly, to the type of water curvature at the surfaces of those water cylinders. This curvature depends, in turn, on the interaction (or surface tension) between the water and the wall material. The removal of extractives from cork seems, therefore, to affect the wall material in such a way that the resulting different shape of the water surface curvature in the lenticels leads to weaker susceptibility effects on the water resonance. This effect is consistent with the extracellular nature of the extractive materials which may, in natural cork, be preferentially located on the surfaces of the lenticular channels.

3.3. Partially desuberised cork

The effects of both non-selective and selective removal of the main hydrophobic component of cork, suberin, on

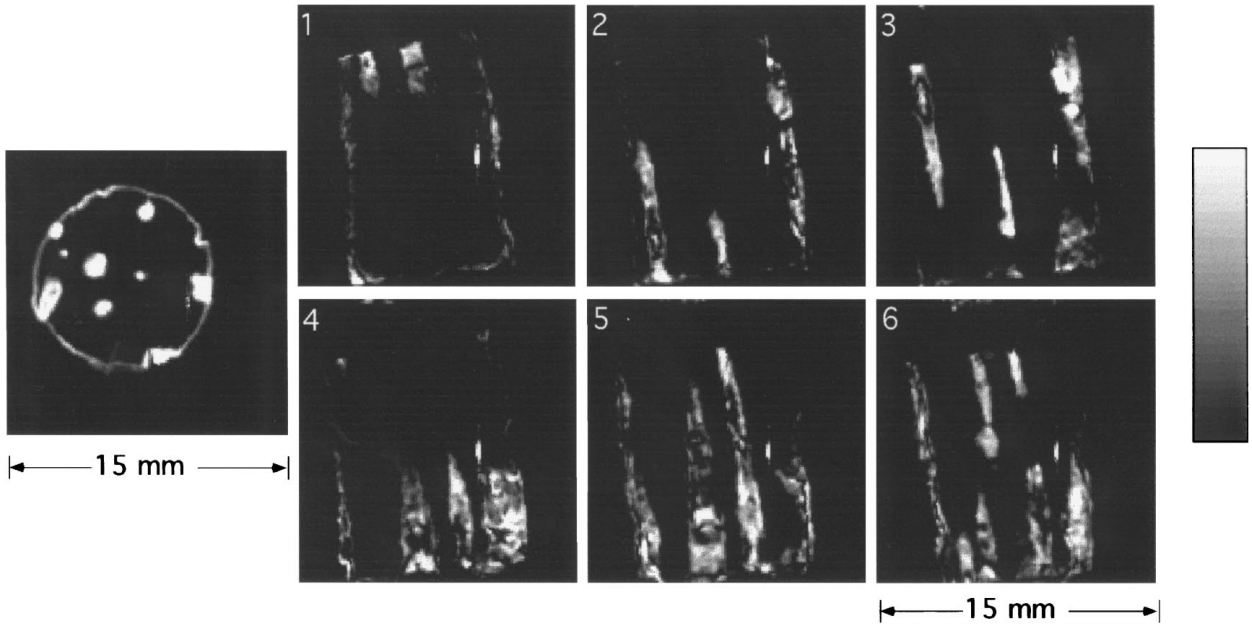

Figure 8 Set of 6 adjacent image slices obtained in the radial section of a sample of extractives-free cork, after soaking in water for 72 hours, along with a single tangential section in the corresponding sample. The lenticular structure is clearly seen. Each slice is 1 mm thick and separated from its neighbours by 1.5 mm. The images are sequential as labelled. As for the natural cork images, shown in Fig. 2, only lenticular and surface water is seen.

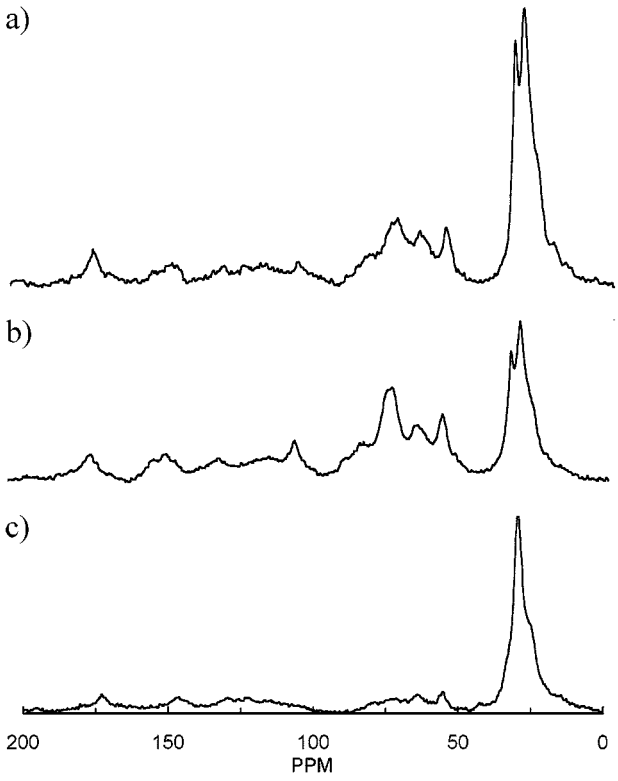

Figure 9 ^{13}C CP/MAS spectra of (a) natural cork and (b) cork after removal of 17% suberin (relatively to 100 grams of cork) with methoxide treatment and (c) cork after selective desuberisation upon heating at 250°C for 20 minutes.

the water absorption properties are described next. Both treatments are based on the structure of the treated cork material, as viewed by ^{13}C NMR [18, 19]. Aliphatic suberin may be easily identified in the ^{13}C CP/MAS spectrum of cork (figure 9a) by the strong peaks at 30 ppm and 33 ppm. Some work has been carried out to investigate the nature of the two peaks and it has been recently proposed [18–20] that 1) the 30 ppm peak arises from mobile suberin chains close to (probably bonded to lignin or lignin-like moieties and 2) the 33 ppm peaks arises from hindered suberin chains close to (probably bonded to) carbohydrate moieties. The removal of suberin by the methoxide treatment has been shown to result in the simultaneous decrease of both suberin peaks [18] Fig. 9b. On the other hand, carefully controlled heating of cork has been shown to result in the preferential degradation of suberin associated with the ^{13}C NMR resonance at 33 ppm, together with carbohydrate [19]. In this work, a cork cylinder was heated at 250°C for 20 minutes and the ^{13}C NMR spectrum of the resulting sample showed the selective disappearance of the 33 ppm peak and the carbohydrate peaks (Fig. 9c). The effects of both non-selective and selective suberin removal on the water ingression are discussed below.

Fig. 10 shows 6 adjacent image slices obtained in the tangential section of a cork sample from which 17% of suberin (calculated relatively to 100 grams of cork) was removed non-selectively. The images clearly show that the non-selective removal of suberin from cork results in significant ingress of water to all parts of the sample. This ingress originates a mass increase about 3.5–4 times greater than for natural cork. Fig. 3d shows that the conditions of alkaline treatment used here enable the cell structure to be partially maintained, although affected by heavy corrugation and local cell breakage (shown as dark patches in figure 3d). Removal of higher amounts of suberin was observed to cause complete degradation of cellular integrity (results not shown), as expected in view of previously results [21]. A similar complete degradation effect was observed for the sample without 17% suberin, after water absorption and subsequent air-drying, preventing a satisfactory microscopic image to be obtained. This result showed that the partially degraded cellular system resulting from

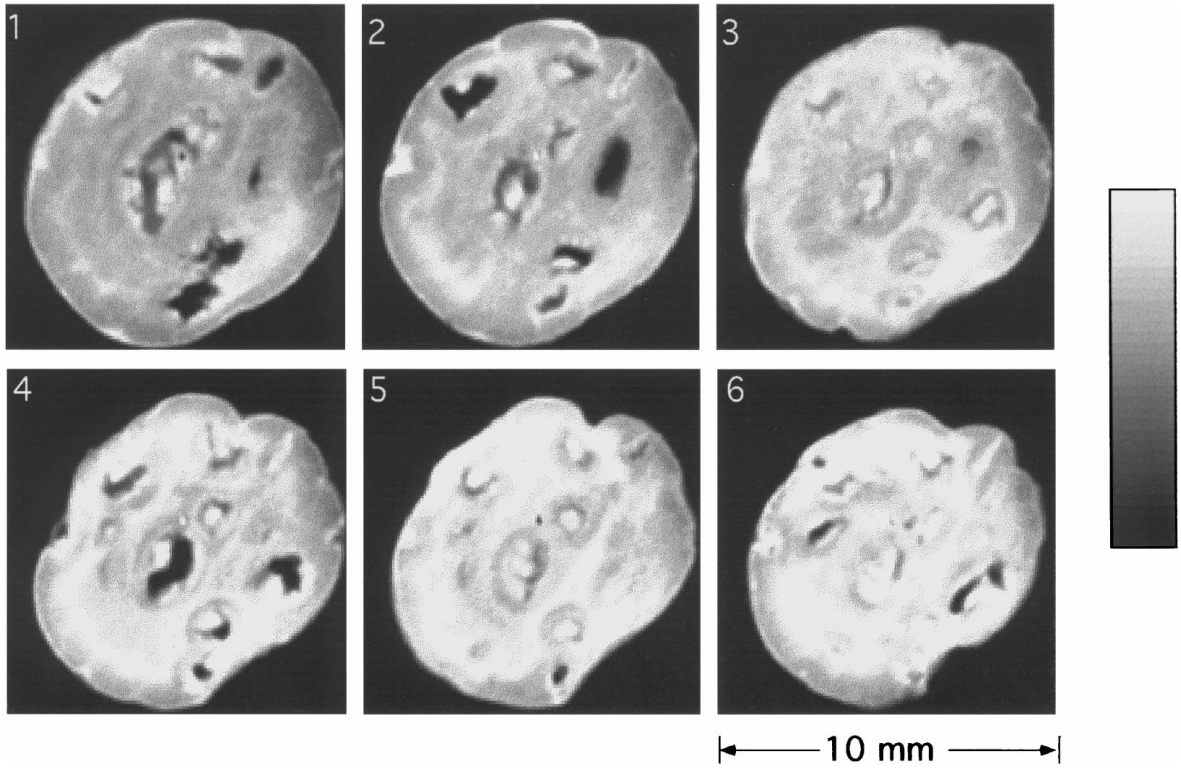

Figure 10 Set of 6 adjacent image slices obtained in the tangential section of nonselective desuberised cork (17% suberin removed), after soaking in water for 72 hours. This image was obtained at a 16 × smaller receiver gain from those shown in Figs 2 and 4 and thus, the grey scale represents a much higher signal water level.

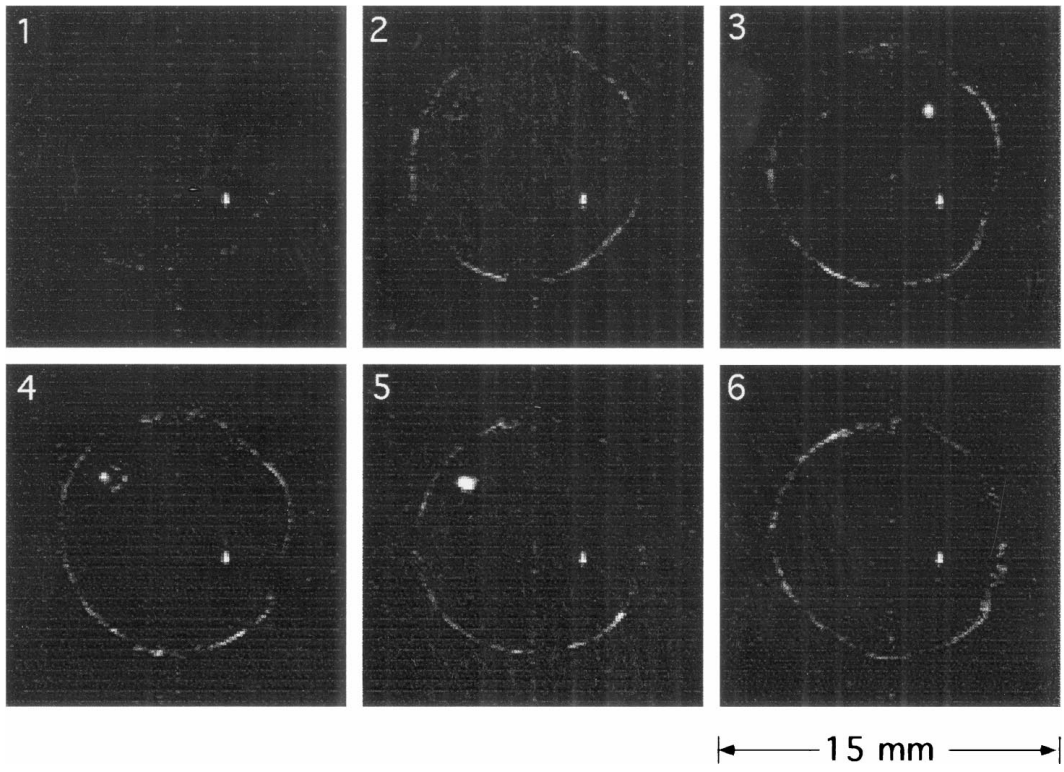

Figure 11 Set of 6 adjacent image slices obtained in the tangential section of a partially desuberised cork sample (33 ppm suberin removed only), after soaking in water for 72 hours. These images were obtained using the same receiver gain as shown in figures 2 and 4. As with the natural cork, only lenticular and surface water can be observed.

the alkaline treatment used (Fig. 3d) was too fragile to resist the effects of hydration and drying. In the proton spectrum (Fig. 5c) of the soaked sample without 17% suberin, the high amount and mobility of water are expressed by the increase in intensity and resolution of the water peak. It should also be noted, however, that the highfield shoulder observed in the MAS spectrum of natural cork (insert in Fig. 5a) has become more prominent in the static spectrum of partially desuberised cork (insert in Fig. 5c). This is consistent with the reported mobility increase of the remaining suberin, as alkaline desuberisation proceeds [18]. Such mobility increase

should lead to both lengthening of T_2 and partial averaging of the anisotropic line broadening contributions.

With basis on these results, we believe that the water ingress observed after non-selective desuberisation of cork is most likely explained by cell-wall damage, rather than by the sole effects of removing part of the hydrophobic component.

Having established the effect of non-selective removal of suberin on the water absorption properties of cork, the effect of selective desuberisation was investigated. Fig. 11 shows 6 adjacent image slices in the tangential section of the selectively desuberised cylinder, clearly indicating a very similar behaviour to that of natural cork and extractive-free cork (Figs 2 and 3). With water only occupying the lenticular channels which, in the sample shown in Fig. 11, were present in a lesser number. It was also clear from the corresponding confocal microscopic image (not shown) that the cell structure is hardly affected by the removal of 33 ppm suberin plus carbohydrate. These interesting results show, therefore, that the particular component of suberin remaining after selective treatment and represented by the 30 ppm peak in the ^{13}C CP/MAS spectrum of cork (Fig. 9) is responsible for the water-insulating properties of cork. The role played by the 30 ppm suberin may result either from it holding together the cell structure, or from conferring a sufficiently hydrophobic character, or from an interplay of both effects. In addition, it should be noted that the above 30 ppm suberin type has been suggested to compose most of the aliphatic suberin fraction of cork whereas the 33 ppm suberin should comprise only a few percent of cork weight. The role played by the former suberin type may therefore be strongly related to its higher content.

4. Conclusion

It has been generally believed that the hydrophobic components of cork, extractives and suberin, must be those responsible for the low absorption of water by that material. In the present work, we established that the extractives fraction has little influence in determining the impermeability of cork to water. On the other hand, the non-selective removal of suberin was shown to lead to immediate and extensive water ingression. The confocal microscopic results shown here confirmed the previously noted importance of suberin in holding together the cell wall structure [12, 16]. We believe that the structural collapse brought about by removing suberin non-selectively is the main explanation for the subsequent water ingression, rather than the decrease in content of that hydrophobic component. Finally, the selective removal of the type of suberin which resonates at 33 ppm in the ^{13}C CP/MAS spectrum of cork, was shown to result in no disruption of cellular structure and in no more water ingression than for natural cork. It is, therefore, concluded that the suberin type which comprises chains resonating at 30 ppm in the ^{13}C NMR spectrum and is known to be located near lignin or lignin-like moieties, is the cork component responsible for the water-insulating properties of that material, either by maintaining the integrity of cellular structure or by conferring enough hydrophobicity to the material.

NMR microscopy was here demonstrated to be a suitable non-invasive technique to probe water ingression and distribution in cork. As well as providing a rapid means of characterising the network of lenticels in a 3D sample of cork, proton NMR was shown to be sensitive to the particular location of the water in the sample of natural cork. In fact, inner water and surface water were shown to have distinct NMR spectral properties thus potentially enabling the monitoring of water ingress in the cork sample.

Acknowledgements

AMG, CPN and MHL acknowledge JNICT-PRAXIS XXI for partial funding of this work (BD/3765/94). PTC acknowledges financial support from the New Zealand Foundation for Research, Science and Technology. The authors are grateful to Dr. R. E. Rowland and Mrs. E. Nickless for making the confocal laser images of the cork samples.

References

1. H. PEREIRA, *Wood Sci. Tech.* **22** (1988) 211.
2. P. J. KOLLATUKUDY, *Science* **208** (1980) 990.
3. P. J. HOLLOWAY, *Phytochemistry* **22** (1983) 495.
4. M. ARNO, M. C. SERRA and E. SEOANE, *Anales de Quimica* **77** (1981) 82.
5. N. CORDEIRO, M. N. BELGACEM, A. J. D. SILVESTRE, C. PASCOAL NETO and A. GANDINI, *Int. J. Biol. Macromol.* **22** (1998) 71.
6. M. A. BERNARDS, M. L. LOPEZ, J. ZAJICEK and N. G. LEWIS, *J. Biol. Chem.* **270** (1995) 7382.
7. B. PERRA, J. P. HALUK and M. METCHE, *Holzforschung* **47** (1993) 486.
8. A. V. MARQUES, H. PEREIRA, D. MEIER and O. FAIX, *ibid.* **48**(suppl) (1994) 43.
9. C. PASCOAL NETO, N. CORDEIRO, A. SECA, F. DOMINGUES, A. GANDINI and D. ROBERT, *ibid.* **50**(6) (1996) 563.
10. M. LOPES, C. PASCOAL NETO, D. EVTUGUIN, A. J. D. SILVESTRE, A. GIL, N. CORDEIRO and A. GANDINI, *ibid.* **52**(2) (1998) 146.
11. O. BORG-OLIVIER and B. MONTIES, *Phytochemistry* **32** (1993) 601.
12. A. E. ROSA and M. A. FORTES, *Wood and Fiber Science* **25**(4) (1993) 339.
13. N. CORDEIRO, C. PASCOAL NETO, A. GANDINI and M. N. BELGACEM, *J. Coll. Inter. Sci.* **174** (1995) 246.
14. N. CORDEIRO, P. AURENTY, M. N. BELGACEM, A. GANDINI and C. PASCOAL NETO, *ibid.* **187** (1997) 498.
15. P. T. CALLAGHAN, "Principles of Nuclear Magnetic Resonance Microscopy" (Oxford Science Publications, Oxford, 1991).
16. A. LEWIS, in "New Techniques of Optical Spectroscopy and Microspectroscopy," edited by R. J. Cherry (The Macmillan Press Ltd, London, 1991) Ch. 2 p. 49.
17. M. A. FORTES, *European Review* **1**(2) (1993) 189.
18. A. M. GIL, M. LOPES, J. ROCHA and C. PASCOAL NETO, *Int. J. Biol. Macromol.* **20** (1997) 293.
19. C. PASCOAL NETO, J. ROCHA, A. GIL, N. CORDEIRO, A. P. ESCULCAS, S. ROCHA, I. DELGADILLO, J. D. PEDROSA DE JESUS and A. J. FERRER CORREIA, *Soli. St. Nucl. Mag. Reson.* **4** (1995) 143.
20. M. H. LOPES, A. SARYCHEV, C. PASCOAL NETO and A. M. GIL, *Solid State NMR*, in press.
21. H. PEREIRA and A. V. MARQUES, *IAWA Bulletin n.s.* **9**(4) (1988) 337.

Received 2 March
and accepted 16 August 1999